Article

Chemical Reactive and Viscous Dissipative Flow of Magneto Nanofluid via Natural Convection by Employing Galerkin Finite Element Technique

Shankar Goud Bejawada [1], Wasim Jamshed [2], Rabia Safdar [3], Yanala Dharmendar Reddy [4], Meznah M. Alanazi [5], Heba Y. Zahran [6,7] and Mohamed R. Eid [8,9,*]

[1] Department of Mathematics, JNTUH College of Engineering Hyderabad Kukatpally, Hyderabad 500085, Telangana, India; bsgoud.mtech@gmail.com

[2] Department of Mathematics, Capital University of Science and Technology (CUST), Islamabad 44000, Pakistan; wasiktk@hotmail.com

[3] Department of Mathematics, Lahore College for Women University, Lahore 54000, Pakistan; rabia.safdar1109@gmail.com

[4] Department of Mathematics, Anurag University, Venkatapur, Hyderabad 500088, India; dharmayanala@gmail.com

[5] Department of Physics, College of Science, Princess Nourah bint Abdulrahman University, P.O. Box 84428, Riyadh 11671, Saudi Arabia; mmalenazy@pnu.edu.sa

[6] Laboratory of Nano-Smart Materials for Science and Technology (LNSMST), Department of Physics, Faculty of Science, King Khalid University, P.O. Box 9004, Abha 61413, Saudi Arabia; heldemardash@kku.edu.sa

[7] Nanoscience Laboratory for Environmental and Biomedical Applications (NLEBA), Metallurgical Lab. 1, Department of Physics, Faculty of Education, Ain Shams University, Roxy, Cairo 11757, Egypt

[8] Department of Mathematics, Faculty of Science, New Valley University, Al-Kharga 72511, Al-Wadi Al-Gadid, Egypt

[9] Department of Mathematics, Faculty of Science, Northern Border University, Arar 1321, Saudi Arabia

* Correspondence: m_r_eid@yahoo.com

Abstract: A numerical study of chemically reactive effects on Magnetohydrodynamics (MHD) free convective unsteady flowing over an inclined plate in a porousness material in the existence of viscous dissipation was studied. The nondimensional principal equations are time dependent coupled and non-linear partial differential equations (PDEs) are solved by the efficacy finite element method (FEM). As well, the computational relationships of speed, energy, and concentricity in the form of Galerkin finite element were obtained. Calculations are achieved with a wide range of key flow parameters, namely, the angle of inclination (α), permeability parameter (k), magnetic parameter (M), buoyancy ratio parameter (N), Schmidt number (Sc), Eckert number (Ec), Prandtl number (Pr), chemical factor (Kr) on speed, and concentricity and temperature fields are examined in detail with the assistance of diagrams.

Keywords: inclined plate; MHD; heat and mass transport; chemically reactive species; finite-element method

1. Introduction

Analysis of heat transport due to the continuous increase of surrounding fluid is an application of the present study. Its implementation is in the broader fields of science, particularly in the field of substance designing. In many chemical engineering developments, such as metallurgical developments, the polymer expulsion process includes cooling the melted liquid that has expanded in the cooling system. The industrial use of heat transfer fluids varies from simple, dry design to advanced-sized systems that perform many functions in the production process. As there are many variations in the formulation and application of processes in the usage of heat transport liquids, the sum of the industries

that use this method is large. Miniaturization has had a huge impact on the technology of heat exchangers and now converts heat exchangers into integrated and efficient ones.

Ishak et al. [1] investigated heat transmission across a time dependent stretched plate using a constant heat flow. Palani and Srikanth [2] examined MHD flowing through a semi-infinite perpendicular wall with mass transmission. Muthucumaraswamy and Ganesan [3] discussed mass transfer effects on structures with varying surface heat flow. Elbashbeshy [4] studied heat and mass transmission down an upright wall with varying wall tightness and concentration with a magnetic field. Das et al. [5] examined the finite-difference analysis of the mass transmission influences on flowing through an endless upright sheet that was impulsively initiated in a dissipative fluid with continuous heat flux. Shankar Goud [6] explored the consequences of mass sucking on MHD boundary layer flowing and heat transport via a permeable diminishing plate with a heat generating (sinking).

An enormous exchange is the vehicle of an article (mass) into fluids and gases. Contingent upon the conditions, the climate, and the powers liable for mass exchange, the four fundamental sorts are characterized: (1) circulation in a tranquil climate, (2) mass exchange through a laminar stream, (3) mass exchange through a fierce stream, and (4) mass trade. Many transmissions are used in different fields of science with different processes and methods. Crane [7] studied the flowing past a stretching wall. Dandapat et al. [8] discussed the permanence of MHD flowing of a visco-elastic liquid via an elongating wall. Raju and Sandeep [9] discussed heat (mass) transmission in MHD Casson liquid across a non-linear penetrable elongating side. Elbashbeshy [10] investigated heat transmission across a non-linear elongating continuous surface with sucking. Magyari and Keller [11] studied heat/mass transmission in the boundness layer on a nonlinear extending continuous plane. As a result, various more investigations on natural convection across a stretched wall have been conducted, including the works [12–16].

The investigation of a limit stream and hotness moving over an expandable sheet has gotten a lot of consideration because of its numerous viable applications, such as paper creation, thermal wrapping, plastic filming, adhesive and copper wire, and metal weldings. Elbashbeshy and Bazid [17] likewise explored the warm limit layer in a period subordinate stream (utilizing a limitless foundation) over an unsound surface. Ishak et al. [18] concentrated on heat moving in a lengthy, shaky climate with a consistent divider temperature. The consequences of radiative fluxing on the flowing and transport of heat in an extended unstable area with interior heat-generating were analysed by Abd El-Aziz [19]. Shateyi and Motsa [20] inspected the impact of thermal radiative on heat (mass) transmission across an unstable stretched surface.

Magnetohydrodynamics (MHD) studies the field of magnetism and electrical behaviour. Examples of magneto fluid include plasma, metals, salts, and electrolytes. The first order of the chemical reaction of the unbalanced flow that exceeds the long straight oscillatory plate is calculated at the converted temperature and the same weight difference. Magneto fluid is already widely used in MHD cases. The basic premise of MHD is that the magnets can absorb the undercurrents in the running liquid, it dissipates the liquid and alters the magnetic force. The mathematical set describing MHD is a combination of the Navier–Stokes liquid calculation and Maxwell's electromagnetism calculations. These different calculations should be solved simultaneously by analysis or by numbers. Raptis [21] studied the causes of radiative fluxing on magneto flowing via an upright wall. Ali et al. [22] explored the natural convective MHD flowing via an upright lamina inserted in an absorbent medium. Kim [23] discussed a time dependent magneto convection heat transmission gone a semi-limitless upright penetrable move platter with varying suck. Interestingly, several types of research on MHD flowing have been published in the literature [24,25].

Viscous heat dissipative is the generation of heat through the dynamic (or merely dispersed) combination of streaming heat and thermodynamic (Mase, 1973). The idea comes from a variety of factors, including plate tectonics and mantle convection. The presence of viscous dissipation at the flow level shows a significant role in the high viscosity

of liquids such as polymers and oils. The consequence of viscous degradation on natural convection is commendable when the advertised kinetic energy is reflected in the relative temperature transfer. Over the past two decades, major determinations have been made to regulate fluid flow through sheets to provide important definitions for conventional production and manufacturing procedures, like polymers production, papers creation, food preservation progressions, crystal production, and petrol filtration operations. The first contributions to this area of study were opened to examine the flow of water due to the expanded area by Sakiadis [26]. Mohammadein and Gorla [27] examined the heat transmission structures of the solid level of the micro-polar boundary layer across an expandable, continuous sheet. For more details on this topic, Rasool et al. [28] investigated the entropy production and impacts of binary-chemically reactive on the flow of MHD nanofluid flowing across a nonlinear expanding plate. Chamkha and Khaled [29] inspected the joint mass/heat transmission by free convective flowing via a penetrable wall immersed in a liquid filled absorbent material. Krishna et al. [30] probed the effects of ion slip and Hall on time dependent magneto convective rotational flowing of a heat-producing/engrossing 2nd-grade liquid. Krishna et al. [31] researched the previously same influence but via a nonlinear accelerating lamina in an absorbent substance. Krishna et al. [32] examined the same but by utilizing an elastic/viscous liquid at this time. Wakif et al. [33] examined novel scientific visions into the thermodynamic irreversibility of dissipation electromagnetic liquid currents through a turning horizontal Riga lamina in the presence of sucking and Ohmic heating affects. Kumar et al. [34] investigated Cattaneo/Christov heat transport in Reiner&Philippoff liquid with an oblique magnetic force. Modather et al. [35] explored the oscillatory flowing of a micropolar fluid through an upright penetrable lamina in an absorbent material using an analytical analysis. Takhar et al. [36] considered MHD flow over a moving plate in a rotating fluid, including MHD and Hall-fluxes with ambient speed. Chamkha [37] characterized the effects of radiative fluxing and resilience on MHD flowing across an accelerating penetrable side with a heat generating (sinking). Takhar et al. [38] examined unsteady flowing and heat transmission on a semi-limitless flatness lamina with an associated magnetically force. For further information on this topic, see [39–52] and the cross-references listed therein.

Through the previous studies presented above, we found that the effect of chemical interaction and magnetohydrodynamic unsteady flowing by free convection in the presence of viscous dissipation on a plate tilted at an angle α in an absorbent material has not been inspected. The current work is being done to analyze the computational studies by developing the Galerkin-FEM of the chemically interactive influences on MHD natural convective flowing across a slanted surface in the presence of viscidness dissipative in a penetrable material. The benefit of FEM is that it is uncomplicated, compressed, and conclusions-orientated, creating it very prevalent in the scientific and engineering societies. Furthermore, numerical results of speed, energy, and concentricity in the form of Galerkin finite element were obtained.

2. Physical and Mathematical Background

Consider the unstable flow of non-compressed viscous liquid driven by an inclined plate to a fixed temperature at the same temperature T'_w that responds to chemicals and viscous dispersion. The axis x' is considered horizontal to the lamina, $y'-$ axis is considered normal on the plate, and magnetic force of consistent B_0 is employed in y' path (Figure 1a). At $t' > 0$ the plate temperature rises to T'_w and focuses on C'_w. All terms in the control numbers will be independent of x' with no flow in line with the y' direction. It is considered that no voltage is supplied, implying the lack of an electromagnetic current. The transverse affected magnetic force and magnetically Reynolds amounts are assumed to be extremely little so that the generated magnetic force and the Hall cause are negligible.

Then, underneath the typical Boussinesq's approximations with the boundary layer, the governing formulas are:

$$\frac{\partial u'}{\partial y'} = 0 \tag{1}$$

$$\frac{\partial u'}{\partial t'} = \nu \frac{\partial^2 u'}{\partial y'^2} + g\beta(T' - T'_\infty) + g\beta'(C' - C'_\infty) - \nu \frac{u'}{k'} - \frac{\sigma B_0^2}{\rho} u' \tag{2}$$

$$\frac{\partial T'}{\partial t'} = \frac{k}{\rho C_p} \frac{\partial^2 T'}{\partial y'^2} + \frac{\mu}{\rho C_p} \left(\frac{\partial u'}{\partial y'} \right)^2 \tag{3}$$

$$\frac{\partial C'}{\partial t'} = D \frac{\partial^2 C'}{\partial y'^2} - K'_r(C' - C'_\infty) \tag{4}$$

and the applicable boundary restrictions are

$$\left. \begin{array}{l} t' \leq 0 : u' = 0,\ T' = T'_\infty, C' = C'_\infty \quad for\ all\ y' \geq 0, \\ t^* > 0 : \begin{cases} u' = 0,\ T' = T'_\infty, C' = C'_\infty & at\ y' = 0 \\ u' \to 0,\ T' \to T'_\infty, C' \to C'_\infty & as\ y' \to \infty \end{cases} \end{array} \right\} \tag{5}$$

and we introduce the non-dimensional variables, as follows

$$\left. \begin{array}{l} u = \{\nu g(T'_w - T'_\infty)\}^{\frac{1}{3}}, u_0 = \{\nu g\beta(T^*_w - T^*_\infty)\}^{\frac{1}{3}}, y = \left\{ \frac{\nu g(T'_w - T'_\infty)}{\nu^2} \right\}^{\frac{1}{3}}, \\ t = \left\{ \frac{g^2\beta^2(T'_w - T'_\infty)^2}{\nu} \right\}^{\frac{1}{3}}, M = \frac{\sigma B_0^2 \nu}{u_0^2 \rho}, \ k = \frac{\nu^2}{\nu_0^2 k'}, \ Pr = \frac{\nu \rho C_p}{k} = \frac{\nu}{\alpha}, \\ N = \frac{\beta^*(C' - C'_\infty)}{\beta(T' - T'_\infty)}, Sc = \frac{\nu}{D}, \ Kr = \frac{K'_r \nu}{\nu_0^2} t_0, \theta = \frac{T' - T'_\infty}{T'_w - T'_\infty}, \ C = \frac{C' - C'_\infty}{C'_w - C'_\infty}. \end{array} \right\} \tag{6}$$

According to relations (1–4) with (6), the governance formulas are changed to

$$\frac{\partial u}{\partial t} = \frac{\partial^2 u}{\partial y^2} + \theta cos\alpha + NC cos\alpha - \left(\frac{1}{K} + M \right) u \tag{7}$$

$$\frac{\partial \theta}{\partial t} = \frac{1}{Pr} \frac{\partial^2 \theta}{\partial y^2} + Ec \left(\frac{\partial u}{\partial y} \right)^2 \tag{8}$$

$$\frac{\partial C}{\partial t} = \frac{1}{Sc} \frac{\partial^2 C}{\partial y^2} - KrC \tag{9}$$

The boundary and preliminary restrictions are

$$\left. \begin{array}{l} t \leq 0 : u = 0,\ \theta = 0, C = 0 \quad for\ all\ y \geq 0, \\ t > 0 : \begin{cases} u = 0,\ \theta = 1, C = 1 & for\ all\ y \geq 0\ at\ y = 0, \\ u \to 0,\ \theta \to 0, C \to 0 & as\ y \to \infty. \end{cases} \end{array} \right\} \tag{10}$$
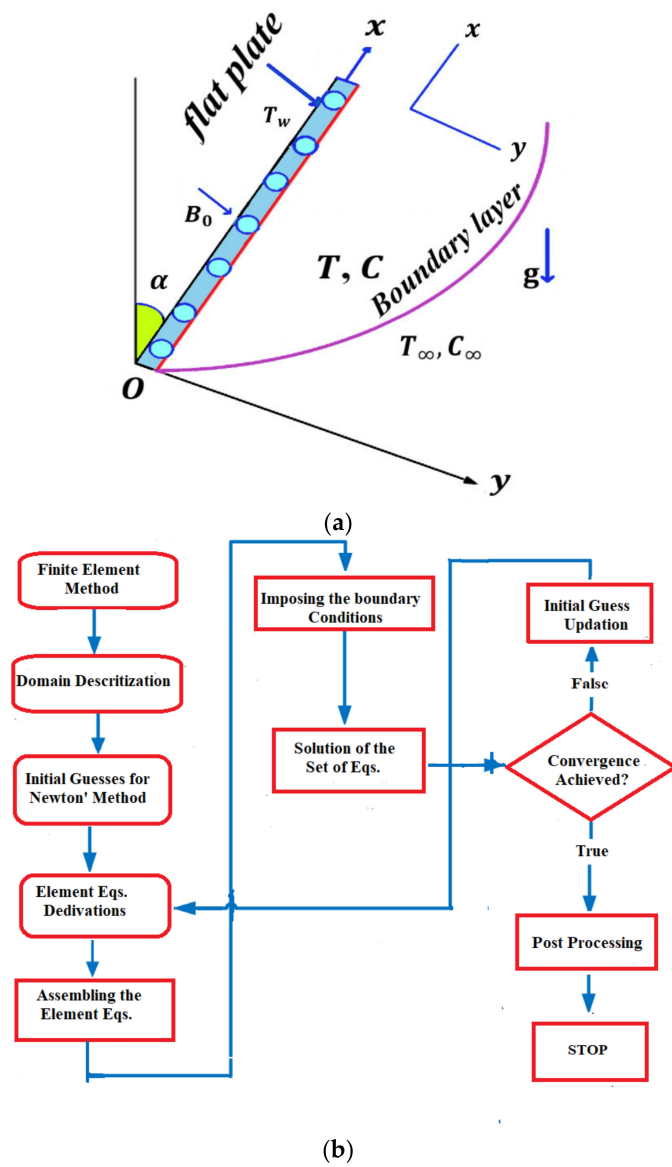
(a)

(b)

Figure 1. (**a**) Geometry of the model. (**b**) Solution of the model flow chart.

3. Solution of the Problem

To obtain numerical solutions for Equations (7) and (8) under the boundary conditions of (10), FEM has been used and can be seen in the solution of the problem flow chart in Figure 1b. Many integrated, indirect degree separation systems can be solved using this process because it is very efficient and allows for robust solutions.

Using the Galerkin-FEM to solve Equation (7) around the constituent (e), $y \epsilon \left[y_j, y_k \right]$ is:

$$\int_{y_j}^{y_k} \left\{ N^{(e)T} \left[\frac{\partial^2 u^{(e)}}{\partial y^2} - \frac{\partial u^{(e)}}{\partial t} - B u^{(e)} + R_1 \right] \right\} dy = 0 \qquad (11)$$

where $R_1 = \theta \cos\alpha + CN \cos\alpha$, $B = \left(B + \frac{1}{K} \right)$.

When the integrating by parts methods is applied to the first term of Equation (11), the following results:

$$N^{(e)^T} \left\{ \frac{\partial u^{(e)}}{\partial t} \right\}_{y_j}^{y_\kappa} - \int_{y_j}^{y_\kappa} \left\{ \frac{\partial N^{(e)^T}}{\partial y} \frac{\partial u^{(e)}}{\partial y} - N^{(e)^T} \left[\frac{\partial u^{(e)}}{\partial t} + Bu^{(e)} - R_1 \right] \right\} dy = 0 \qquad (12)$$

By neglecting the initial bound from relation (12) and put the linear-piecewise estimate speed relation be $u^{(e)} = N_j(y)u_j(t) + N_\kappa(y)u_\kappa$ and $(t) = N_j u_j + N_\kappa u_j$, here $N_j = \frac{y_\kappa - y}{y_\kappa - y_j}$ and $N_\kappa = \frac{y - y_j}{y_\kappa - y_j}$ are the essential relationships, $N^{(e)^T} = \begin{bmatrix} N_j & N_\kappa \end{bmatrix}^T = \begin{bmatrix} N_j \\ N_k \end{bmatrix}$ across the component (e). By reducing and considering the subsequent combined elements $y\epsilon[y_{i-1}, y_i]$ and $y\epsilon[y_i, y_{i+1}]$, so adjusting the row corresponding to the node "i" to zero, we acquire:

$$\frac{1}{h^2}[-u_{i-1} + 2u_i - u_{i+1}] + \frac{1}{6}[\dot{u}_{i-1} + 4\dot{u}_i + \dot{u}_{i+1}] + \frac{B}{6}[u_{i-1} + 4u_i + u_{i+1}] = R_1 \qquad (13)$$

The Crank–Nicolson technique generates the following system of equations when the trapezoidal rule is used:

$$A_1 u_{i-1}^{n+1} + A_2 u_i^{n+1} + A_3 u_{i+1}^{n+1} = A_4 u_{i-1}^n + A_5 u_i^n + A_6 u_{i+1}^n + R_1, \qquad (14)$$

where $A_1 = A_3 = 2 - 6r + B\kappa$, $A_2 = 8 + 12r + 4B\kappa$,
$A_4 = A_6 = 2 + 6r - B\kappa$, $A_5 = 8 - 12r - 4B\kappa$, and $R_1 = \theta \cos\alpha + CN \cos\alpha$.
The following equations may now be deduced from Equations (8) and (9):

$$B_1 \theta_{i-1}^{n+1} + B_2 \theta_i^{n+1} + B_3 \theta_{i+1}^{n+1} = B_4 \theta_{i-1}^n + B_5 \theta_i^n + B_6 \theta_{i+1}^n + R_2, \qquad (15)$$

$$C_1 C_{i-1}^{n+1} + C_2 C_i^{n+1} + C_3 C_{i+1}^{n+1} = C_4 C_{i-1}^n + C_5 C_i^n + C_6 C_{i+1}^n, \qquad (16)$$

where $B_1 = B_3 = Pr - 3r$, $B_2 = 4Pr + 6r$, $B_4 = B_6 = Pr + 3r$, $B_5 = 4Pr - 6r$, $C_1 = C_3 = 2Sc + \kappa ScKr - 6r$, $C_2 = 8Sc + 12r + 4\kappa ScKr$, $C_4 = C_6 = 2Sc - \kappa ScKr + 6r$, $C_5 = 8Sc - 4kKrSc - 12r$, and $R_2 = 12Ec\kappa \left(\frac{\partial u_i}{\partial y_i} \right)^2$.

Here, $r = \frac{\kappa}{h^2}$ and (h, κ) denotes the mesh size along y and t time directions, respectively. The index 'i' relates to space, whereas the index 'n' corresponds to time (t). Taking $i = 1 \ldots, m$ and employing the boundary conditions of (10), in Equations (14)–(16), the following system of equations is obtained:

$$A_i X_i = B_i \qquad i = 1 \ldots, m \qquad (17)$$

where A_is are the matrix sizes of m matrices and X_i, B_is are column matrices with m' components. Solutions for the above mathematical systems are determined using Thomas's algorithm in speed, temperature, and concentration. Implementing the MATLAB program also provides statistics. With a small number of (h, κ), Galerkin's moderate feature method is stable and flexible, as no significant changes in speed, temperature, or concentration have been found. Outputs are compared and found to have excellent coherence with the existing literature of Ahmed and Sarmah [48] under induced conditions, which are exhibited in Figure 2 and Table 1.
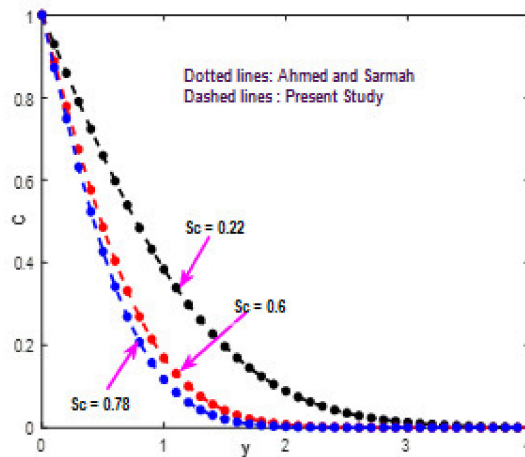
Figure 2. Graphical comparison with [48].

Table 1. Comparing Sherwood number with *Sc* for *Pr* = 0.7.

Sc	Ref. [48]	Present
0.22	0.552791	0.5528
0.6	0.874039	0.8741
0.78	0.996557	0.9966

4. Outcomes and Discussions

The effects of chemically reactions on magneto natural convection flowing over the oblique lamina in with viscidness dissipative was examined. Galerkin's finite method is used to solve outstanding calculations. The parametrical cause of diverse material manifestations on speed, concentration, and energy outlines concerning time t ($t = 0.1$ and $t = 0.15$) is presented in Figures 3–14. These factors include angle of inclination α, permeability parameter k, magnetically parameter M, buoyancy-ratio factor N, Schmidt number Sc, Eckert amount Ec, Prandtl amount Pr, and chemically Interactive factor Kr. Graphical plots are presented to show the influences. The impact regarding the angle of tendency α on the profile of speed for time t is depicted in Figure 3. At time $t = 0.15$, when the increment is done in a parameter of the angle of tendency α, the speed profile is observed to be decreased. Although the same decrement is observed for time $t = 0.1$, the influence obtained is less than those at time $t = 0.15$. The angle of inclination appears to reduce the influence of buoyant force owing to thermal diffusion. As a result, the driving force to the fluid reduces, and the velocity eventually falls.
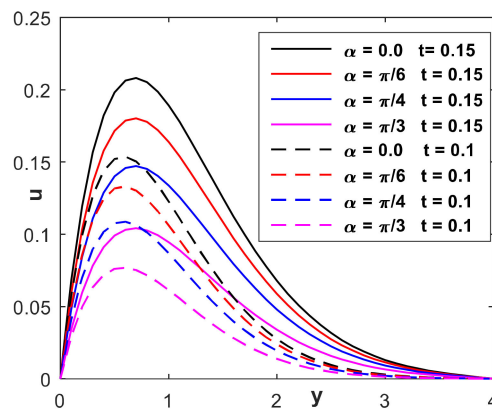

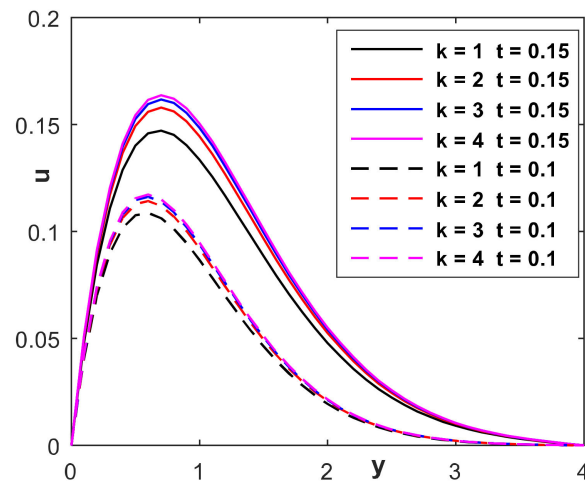**Figure 3.** Velocity sketches for diverse amounts of angle of inclination α.

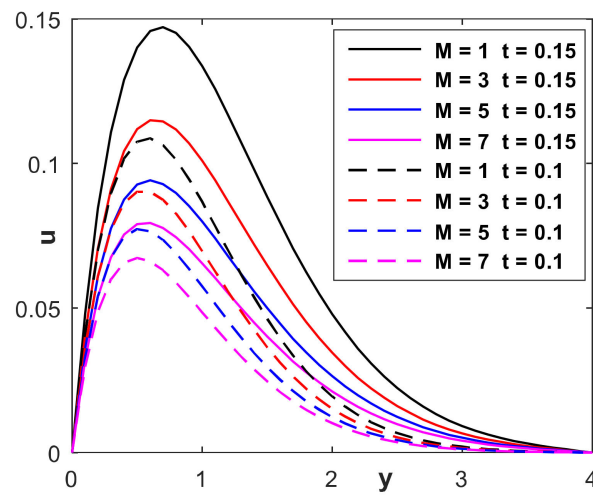**Figure 4.** Velocity sketches for diverse amounts of permeability *k*.

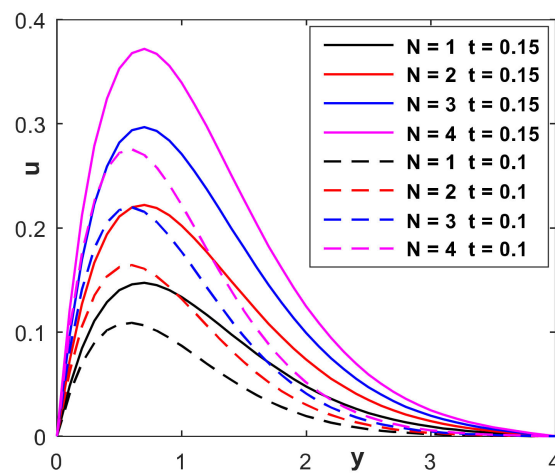**Figure 5.** Velocity sketches for diverse amounts of magnetically factor *M*.

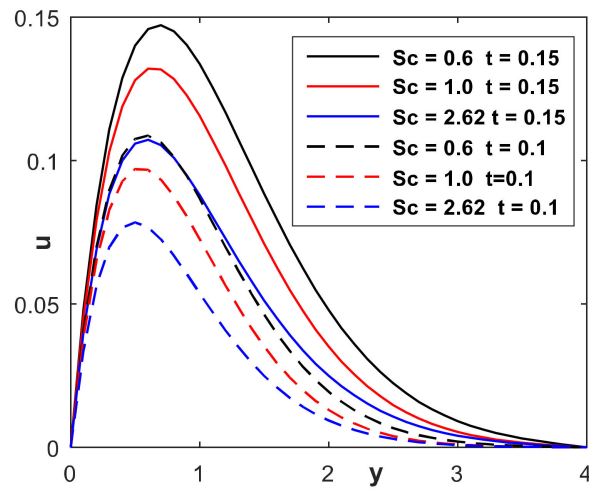**Figure 6.** Velocity sketches for diverse amounts of buoyancy ratio *N*.

Figure 7. Velocity sketches for diverse amounts of Schmidt number *Sc*.
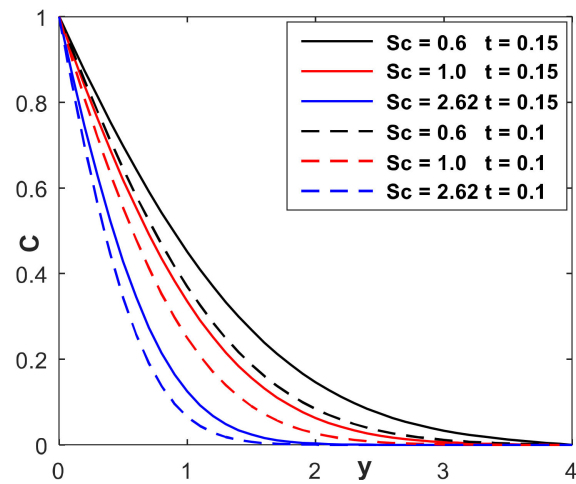
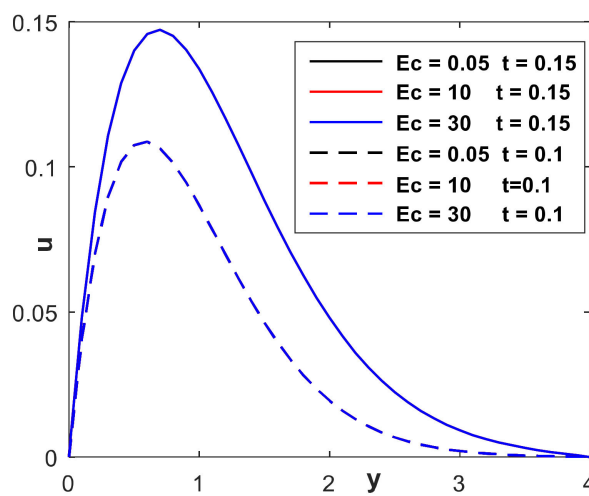**Figure 8.** Concentration sketches for diverse amounts of Schmidt *Sc*.

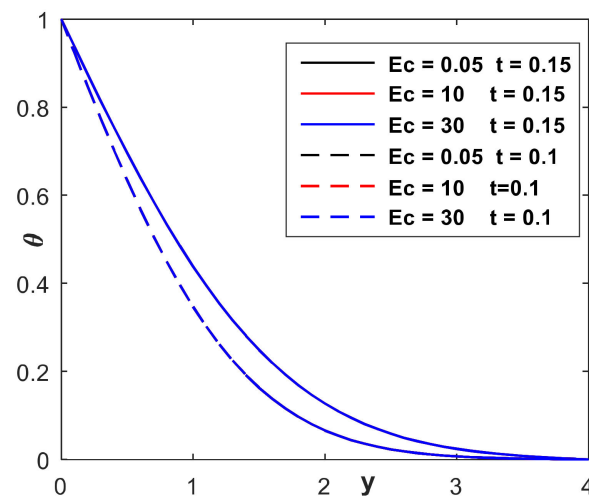**Figure 9.** Velocity sketches for diverse amounts of Eckert *Ec*.

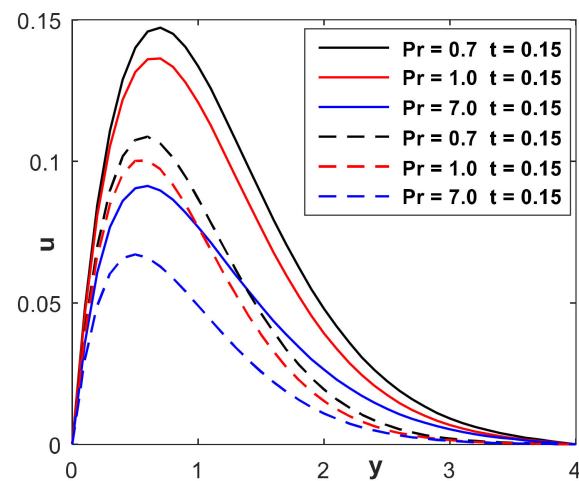**Figure 10.** Temperature sketches for diverse amounts of Eckert *Ec*.

Figure 11. Velocity sketches for diverse amounts of Prandtl *Pr*.
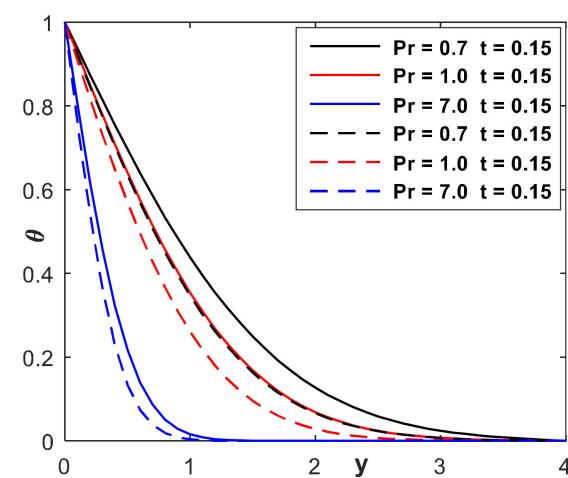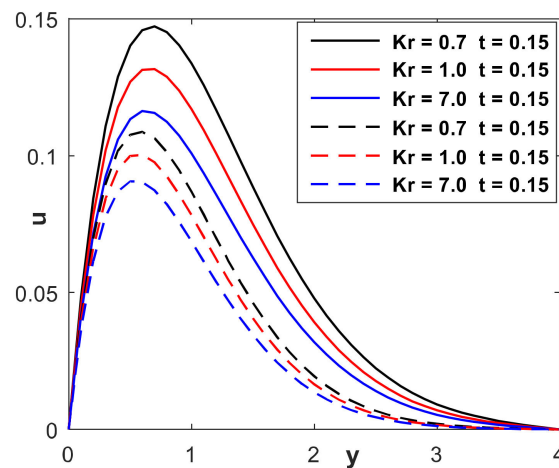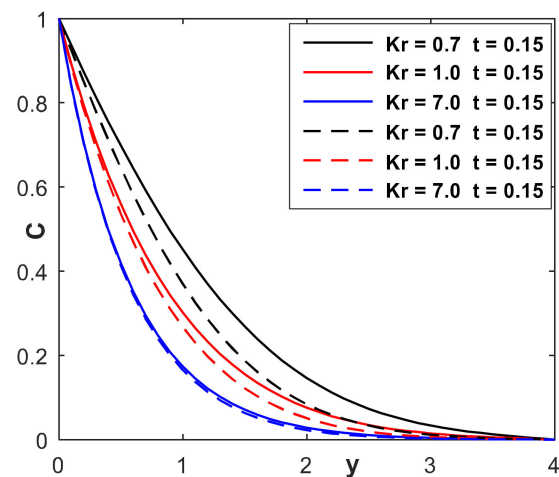

Figure 12. Temperature sketches for diverse amounts of Prandtl *Pr*.

Figure 13. Velocity sketches for diverse amounts of chemical reaction *Kr*.

Figure 14. Temperature sketches for different values of chemical reaction *Kr*.

Figure 4 shows the influence of penetrability constraint *k* on speed profile concerning time *t*. At the start when time $t = 0.15$, a deceleration is obtained in the velocity field, which is a result of the increment in permeability parameter *k*. Meanwhile, the same effect is attained when the time level is changed, i.e., at $t = 0.1$. It is evident that the presence of a porous material supports fluid flow, causing the stream to accelerate after the pores are filled with the fluid. As a result, increasing the impermeability parameter increases resistance and friction to fluid motion and, in this case, velocity. Figure 5 represents the magnetic parameter M's impact on velocity profile for two time levels, $t = 0.15$ and $t = 0.1$. According to the graph, a reduction is obtained in velocity profile with increasing values of magnetic parameter *M* at both time levels. The magnetically field slows liquid motion because magnetization liquid provides a resistive force or skin friction, known as a Lorentz force, which slows electrical transmitted liquid movement. Because the introduction of a crosswise magnetically force produces a resistant-kind strength (Lorentz force) comparable to skin friction, it attempts to impede the liquid motion, lowering its velocity. Figure 6 represents the parametrical impact of the buoyancy ratio *N* on velocity profile for the time levels $t = 0.15$ and $t = 0$. It is noteworthy that the speed profile upsurges as the parameter amount of the buoyancy ratio raises in both periods. Physically, higher *N* values indicate tiny temperature variations.

The effect of the Schmidt number *Sc* on velocity, as well as on concentration profile, at two time levels is depicted in Figures 7 and 8, correspondingly. Figure 7 demonstrates

that once the amount of the Schmidt value is increased, the rapidity field is diminished. Figure 8 shows the behavior of the concentricity profile to be lessened as the Schmidt value is heightened at both times. The Schmidt number *Sc* denotes the fraction of impetus to mass diffusion. It calculates the comparative efficiency of dynamic and mass transfer via transmission in the hydrodynamics (rapidity) and concentricity bounded layers. Increased Schmidt amounts drop the liquid's mass diffuseness, resulting in a drop in concentricity outlines. Figures 9 and 10 show the behavior of the rapidity and energy outlines regarding the Eckert number *Ec*, respectively. Figure 9 depicts the velocity behavior according to the Eckert number *Ec*. When the Eckert number *Ec* is increased, the velocity profile is also increased at both times. Performance of the heat outline for *Ec* is shown in Figure 10. An increment in the Eckert number *Ec* gives an increasing profile of temperature. Because of frictional heating, heat is created in the fluid as the value of *Ec* grows. *Ec* is the physical ratio of kinetic energy to the specific enthalpy difference between the wall and the fluid. As a result, an increasing *Ec* causes the translation of kinetic energy obsessed by interior energy via effort accomplished alongside viscidness liquid forces. As a result, raising the *Ec* raises the temperature of the fluid.

Figures 11 and 12 represent the Prandtl number *Pr*'s impact on profiles of velocity and temperature at times $t = 0.1$ and $t = 0.15$. Figure 11 shows the behavior of the velocity profile according to Prandtl number *Pr*. It is noted that when the *Pr* is heightened, a decrease in the velocity profile is observed at both times. Since a liquid with a small Prandtl number has a large heat diffusion coefficient, it has a higher quantity in the situation of steady. Figure 12 indicates the influence of *Pr* on energy. Boosting *Pr* has led to a reduction in the heat profile at both levels of time. This is because as the Prandtl number upsurges, convective currents weaken and the temperature lowers qualitatively, resulting in a decrease in velocity and concentration. Figures 13 and 14 display the comportment of the rapidity and heat outlines regarding the chemical reaction parameter *Kr*, respectively. According to Figure 13, when the increment is done in the parametrical values of the chemical reaction, the velocity field is decreased. Figure 14 shows the temperature behavior concerning the chemical reaction parameters. Deceleration is obtained in temperature when the rates of the chemical reaction parameter are increased at both time levels. Physically, when the chemically interaction factor rises, it produces the kinematic viscosity to heighten, which in turn causes a decline in molecular diffusions, and, therefore, fluid velocity and concentration diminish.

5. Conclusions

The assumptions were made to study the effect of a chemical reaction and magnetohydrodynamic unsteady fluid flowing by free convection in the presence of viscous dissipation on a plate inclined with an angle α in a porous medium. An excellent agreement was found when comparing our results with the results of previously published studies, and this confirms the reliability and accuracy of the velocity, temperature, and concentration relationships obtained from the finite element method. It is found that the velocity is upsurged with the increment of Eckert number values, buoyancy ratio parameter, and penetrability parameter, and the contrary is observed with the angle of inclination, magnetic field, Schmidt, Prandtl numbers, and chemically Interaction factor. Whilst the heat of the liquid is upsurged at the increment of Eckert numbers, it diminishes when the Prandtl number rises. Concerning the fluid, concentration is reduced by the Schmidt number rising and the chemical reaction parameters.

Nomenclature

g	acceleration due to gravity
$K_r{}'$	dimensional chemical reaction component
C'_∞	the ambient concentrations of the fluid
u', v'	velocity elements at x' and y' axis
B_0	magnetic induction
D	mass diffusion
C_p	specific heat at stabilized pressure
Ec	Eckert number
Pr	Prandtl number
θ	fluid temperature
T'_∞	ambient temperature
α	tendency angle from perpendicular trend
β^*	expansion of concentration coefficient
ρ	liquid density
ν	kinematic viscosity
k	thermal conductivity
β	thermal expansion coefficient
C'_w	concentrations of the fluid
C	dimensionless concentration

References

1. Ishak, A.; Nazar, R.; Pop, I. Heat transfer over an unsteady stretching surface with prescribed heat flux. *Can. J. Phys.* **2008**, *86*, 853–855. [CrossRef]
2. Palani, G.; Srikanth, U. MHD flow past a Semi-infinite vertical plate with mass transfer. *Nonlinear Anal. Model. Control* **2009**, *14*, 345–356. [CrossRef]
3. Muthucumaraswamy, R.; Ganesan, P. Mass transfer effects on impulsively with variable surface heat flux. *Forsch. Ing.* **1999**, *65*, 200–206. [CrossRef]
4. Elbashbeshy, E.M.A. Heat and Mass transfer along a vertical plate with variable surface tension and concentration in the presence of magnetic field. *Int. J. Eng. Sci.* **1997**, *34*, 515–522. [CrossRef]
5. Das, J.N.; Ray, S.N.; Soundalgekar, V.M. Finite difference analysis of mass transfer effects on flow past an impulsively started infinite vertical plate in dissipative fluid and constant heat flux. *Heat Mass Transf.* **1995**, *30*, 155–158. [CrossRef]
6. Shankar, G.B.; Srilatha, P.; Shekar, M.N.R. Effects of mass suction on MHD boundary layer flow and heat transfer over a porous shrinking sheet with heat source/sink. *Int. J. Innov. Tech. Exp. Eng.* **2019**, *8*, 263–266.
7. Crane, L.J. Flow past a stretching plate. *J. Appl. Math. Phys.* **1970**, *21*, 645–647. [CrossRef]

8. Dandapat, B.S.; Holmedal, L.E.; Andersson, H.I. On the stability of MHD flow of a viscoelastic fluid past a stretching sheet. *Acta Mech.* **1998**, *130*, 143–146. [CrossRef]

9. Raju, C.S.K.; Sandeep, N. Heat and mass transfer in magnetohydrodynamic Casson fluid over an exponentially permeable stretching surface. *Eng. Sci. Tech.* **2015**, *19*, 45–52. [CrossRef]

10. Elbashbeshy, E.M.A. Heat transfer over an exponentially stretching continuous surface with suction. *Arch. Mech.* **2001**, *53*, 643–651.

11. Magyari, E.; Keller, B. Heat and mass transfer in the boundary layers on an exponentially stretching continuous surface. *J. Phys. D Appl. Phys.* **1999**, *32*, 577–585. [CrossRef]

12. Shankar, G.B.; Narender, G.; Kumar, R.E. Stagnation point flow through a porous medium towards stretching surface in the presence of heat generation. *Int. J. Eng. Adv. Tech.* **2019**, *9*, 2646–2650.

13. Shankar, G.B.; Khan, Z.H.; Hamid, M. Heat generation/absorption on MHD flow of a micropolar fluid over a heated stretching surface in the presence of the boundary parameter. *Heat Transf.* **2021**, *50*, 6129–6147. [CrossRef]

14. Shankar, G.B.; Nandeppanavar, M.M. Ohmic heating and chemical reaction effect on MHD flow of micropolar fluid past a stretching surface. *Partial Differ. Equ. Appl. Math.* **2021**, *4*, 100104. [CrossRef]

15. Bejawada, S.G.; Reddy, Y.D.; Kumar, K.S.; Kumar, E.R. Numerical solution of natural convection on a vertical stretching surface with suction and blowing. *Int. J. Heat Tech.* **2021**, *39*, 1469–1474. [CrossRef]

16. Mukhopadhyay, S. Unsteady boundary layer flow and heat transfer past a porous stretching sheet in presence of variable viscosity and thermal diffusivity. *Int. J. Heat Mass Transf.* **2009**, *52*, 5213–5217. [CrossRef]

17. Elbashbeshy, E.M.A.; Bazid, M.A.A. Heat transfer over an unsteady stretching surface. *Heat Mass Transf.* **2004**, *41*, 1–4. [CrossRef]

18. Ishak, A.; Nazar, R.; Pop, I. Boundary layer flow and heat transfer over an unsteady stretching vertical surface. *Meccanica* **2009**, *44*, 369–375. [CrossRef]

19. Abd El-Aziz, M. Radiation effect on the flow and heat transfer over an unsteady stretching sheet. *Int. Commun. Heat Mass Transf.* **2009**, *36*, 521–524. [CrossRef]

20. Shateyi, S.; Motsa, S.S. Thermal radiation effects on heat and mass transfer over an unsteady stretching surface. *Math. Probl. Eng.* **2009**, *2009*, 965603. [CrossRef]

21. Raptis, A. Effects of thermal radiation on the MHD flow past a vertical plate. *J. Eng. Therm. Phys.* **2017**, *26*, 53–59. [CrossRef]

22. Ali, F.; Khan, I.; Shafie, S.; Musthapa, N. Heat and mass transfer with free convection MHD flow past a vertical plate embedded in a porous medium. *Math. Probl. Eng.* **2013**, *2013*, 346281. [CrossRef]

23. Kim, Y.J. Unsteady MHD convective heat transfer past a semi-infinite vertical porous moving plate with variable suction. *Int. J. Eng. Sci.* **2000**, *38*, 833–845. [CrossRef]

24. Hayat, T.; Mustafa, M. Influence of thermal radiation on the unsteady mixed convection flow of a Jeffrey fluid over a stretching sheet. *Z. Nat.* **2010**, *65*, 711–719. [CrossRef]

25. Ali, F.M.; Nazar, R.; Arifin, N.M.; Pop, I. MHD stagnation-point flow and heat transfer towards stretching sheet with induced magnetic field. *Appl. Math. Mech.* **2011**, *32*, 409–418. [CrossRef]

26. Sakiadis, B.C. Boundary-layer behavior on continuous solid surfaces: I. Boundary-layer equations for two-dimensional and axisymmetric flow. *AIChE J.* **1961**, *7*, 26–28. [CrossRef]

27. Mohammadein, A.A.; Gorla, R.S.R. Heat transfer in a micropolar fluid over a stretching sheet with viscous dissipation and internal heat generation. *Int. J. Numer. Methods Heat Fluid Flow* **2001**, *11*, 50–58. [CrossRef]

28. Rasool, G.; Zhang, T.; Chamkha, A.J.; Shafiq, A.; Tlili, I.; Shahzadi, G. Entropy generation and consequences of binary chemical reaction on MHD Darcy–Forchheimer Williamson nanofluid flow over non-linearly stretching surface. *Entropy* **2020**, *22*, 18. [CrossRef]

29. Chamkha, A.J.; Khaled, A.A. Hydromagnetic combined heat and mass transfer by natural convection from a permeable surface embedded in a fluid-saturated porous medium. *Int. J. Numer. Methods Heat Fluid Flow* **2000**, *10*, 455–477. [CrossRef]

30. Krishna, M.V.; Ahamad, A.N.; Chamkha, A.J. Hall and ion slip impacts on unsteady MHD convective rotating flow of heat generating/absorbing second grade fluid. *Alex. Eng. J.* **2021**, *60*, 845–858. [CrossRef]

31. Krishna, M.V.; Ahamad, A.N.; Chamkha, A.J. Hall and ion slip effects on unsteady MHD free convective rotating flow through a saturated porous medium over an exponential accelerated plate. *Alex. Eng. J.* **2020**, *59*, 565–577. [CrossRef]

32. Krishna, M.V.; Chamkha, A.J. Hall and ion slip effects on MHD rotating flow of elastico-viscous fluid through porous medium. *Int. Commun. Heat Mass Transf.* **2020**, *113*, 104494. [CrossRef]

33. Wakif, A.; Chamkha, A.; Animasaun, I.L.; Zaydan, M.; Waqas, H.; Sehaqui, R. Novel physical insights into the thermodynamic irreversibilities within dissipative EMHD fluid flows past over a moving horizontal Riga plate in the coexistence of wall suction and joule heating effects: A comprehensive numerical investigation. *Arab. J. Sci. Eng.* **2020**, *45*, 9423–9438. [CrossRef]

34. Kumar, K.G.; Reddy, M.G.; Sudharani, M.V.V.N.L.; Shehzad, S.A.; Chamkha, A.J. Cattaneo-Christov heat diffusion phenomenon in Reiner-Philippoff fluid through a transverse magnetic field. *Phys. A* **2019**, *541*, 123330. [CrossRef]

35. Modather, M.; Rashad, A.M.; Chamkha, A.J. An analytical study of MHD heat and mass transfer oscillatory flow of a micropolar fluid over a vertical permeable plate in a porous medium. *Turk. J. Eng. Env. Sci.* **2009**, *33*, 245–258. [CrossRef]

36. Takhar, H.S.; Chamkha, A.J.; Nath, G. MHD flow over a moving plate in a rotating fluid with magnetic field, Hall currents and free stream velocity. *Int. J. Eng. Sci.* **2002**, *40*, 1511–1527. [CrossRef]

37. Chamkha, A.J. Thermal radiation and buoyancy effects on hydromagnetic flow over an accelerating permeable surface with heat source or sink. *Int. J. Eng. Sci.* **2000**, *38*, 1699–1712. [CrossRef]
38. Takhar, H.S.; Chamkha, A.J.; Nath, G. Unsteady flow and heat transfer on a semi-infinite flat plate with an aligned magnetic field. *Int. J. Eng. Sci.* **1999**, *37*, 1723–1736. [CrossRef]
39. Bejawada, S.G. Thermal radiation influences on MHD stagnation point stream over a stretching sheet with slip boundary conditions. *Int. J. Thermofluid Sci. Tech.* **2020**, *7*, 070201. [CrossRef]
40. Shankar, G.B. Heat generation/Absorption influence on steady stretched permeable surface on MHD flow of a micropolar fluid through a porous medium in the presence of variable suction/injection. *Int. J. Thermofluids* **2020**, *7–8*, 100044. [CrossRef]
41. Shankar, G.B.; Kumar, P.P.; Malga, B.S. Effect of heat source on an unsteady MHD free convection flow of Casson fluid past a vertical oscillating plate in porous medium using finite element analysis. *Partial Differ. Equ. Appl. Math.* **2020**, *2*, 100015. [CrossRef]
42. Bejawada, S.G.; Yanala, D.R. Finite element Soret Dufour effects on an unsteady MHD heat and mass transfer flow past an accelerated inclined vertical plate. *Heat Transf.* **2021**, *50*, 8553–8578. [CrossRef]
43. Shankar, G.B.; Srilatha, P.; Bindu, P.; Krishna, Y.H. Radiation effect on MHD boundary layer flow due to an exponentially stretching sheet. *Adv. Math. Sci. J.* **2020**, *9*, 10755–10761. [CrossRef]
44. Srinivasulu, T.; Shankar, G.B. Effect of inclined magnetic field on flow, heat and mass transfer of Williamson nanofluid over a stretching sheet. *Case Stud. Therm. Eng.* **2021**, *23*, 100819. [CrossRef]
45. Jamshed, W.; Eid, M.R.; Nisar, K.S.; Nasir, N.A.A.M.; Edacherian, A.; Saleel, C.A.; Vijayakumar, V. A numerical frame work of magnetically driven Powell-Eyring nanofluid using single phase model. *Sci. Rep.* **2021**, *11*, 16500. [CrossRef] [PubMed]
46. Shahzad, F.; Baleanu, D.; Jamshed, W.; Nisar, K.S.; Eid, M.R.; Safdar, R.; Ismail, K.A. Flow and heat transport phenomenon for dynamics of Jeffrey nanofluid past stretchable sheet subject to Lorentz force and dissipation effects. *Sci. Rep.* **2021**, *11*, 22924. [CrossRef]
47. Ramzan, M.; Gul, H.; Mursaleen, M.; Nisar, K.S.; Jamshed, W.; Muhammad, T. Von Karman rotating nanofluid flow with modified Fourier law and variable characteristics in liquid and gas scenarios. *Sci. Rep.* **2021**, *11*, 16442. [CrossRef]
48. Ahmed, N.; Sarmah, H.K. Thermal radiation effect on a transient MHD flow with mass transfer past an impulsively fixed infinite vertical plate. *Int. J. Appl. Math. Mech.* **2009**, *5*, 87–98.
49. Safdar, R.; Jawad, M.; Hussain, S.; Imran, M.; Akgul, A.; Jamshed, W. Thermal radiative mixed convection flow of MHD Maxwell nanofluid: Implementation of Buongiorno's model. *Chin. J. Phys.* **2021**. [CrossRef]
50. Koulali, A.; Abderrahmane, A.; Jamshed, W.; Hussain, S.M.; Nisar, K.S.; Abdel-Aty, A.H.; Yahia, I.S.; Eid, M.R. Comparative study on effects of thermal gradient direction on heat exchange between a pure fluid and a nanofluid: Employing finite volume method. *Coatings* **2021**, *11*, 1481. [CrossRef]
51. Redouane, F.; Jamshed, W.; Devi, S.U.; Prakash, M.; Nisar, K.S.; Nasir, N.A.A.M.; Khashan, M.M.; Yahia, I.S.; Eid, M.R. Galerkin finite element study for mixed convection (TiO$_2$-SiO$_2$/Water) hybrid-nanofluidic flow in a triangular aperture heated beneath. *Sci. Rep.* **2021**, *11*, 22905. [CrossRef] [PubMed]
52. Goud B.S.; Reddy, Y.D.; Rao, V.S. Thermal radiation and Joule heating effects on a magnetohydrodynamic Casson nanofluid flow in the presence of chemical reaction through a non-linear inclined porous stretching sheet. *J. Nav. Archit. Mar. Eng.* **2020**, *17*, 143–164. [CrossRef]